CHAPTER 5

Establishment of the Experimental Setup

Characterization of GYF domain binding properties required expression of functional domains in sufficient amounts. Furthermore, the desired experimental set up to define the binding characteristics, a combination of phage display and SPOT analysis, was to be evaluated for its compatibility with this adaptor domain family. The folding status of GYF domain constructs was tested by NMR spectroscopy (Fig. 5.1). Functionality of the domains and compatibility with SPOT analysis were simultaneously assessed. The SPOT test membranes comprised potential ligands. The known interaction between CD2BP2-GYF and CD2 peptides served as a control in this experiment (Fig. 5.2). The binding capacity of the domains in phage display experiments was tested similarly (Fig. 5.3).

5.1 Expression of Functional GYF Domains

Several GYF domains were constructed as His_6-tagged and/or as GST-tagged protein fragments. The GYF domain of CD2BP2 guided domain border selection, but for SMY2 and SYH1, only longer domain constructs were expressed successfully (Table 4.2, Fig. 9.1, and data not shown). NMR spectra of purified His_6-tagged PERQ2- and untagged SMY2-GYF were compared with those of the untagged CD2BP2-GYF and showed that the two SMY2-type GYF domains adopt a folded conformation as well. The ^1H spectra of all three constructs showed broad peak dispersion in the amide region (6–12 ppm) and shifted methyl resonances (below 0 ppm) were observed, indicative of folded domains (Fig. 5.1a, c, and e). Chemical shift dispersion reflects the different chemical environments of hydrogen atoms from individual aromatic, aliphatic or amide groups in a folded domain, compared to the more redundant environment in an non-structured protein (see Chapter 3). Peaks below 0 ppm correspond to methyl-protons in a hydrophobic surrounding, such as the domain core.

In ^1H-^{15}N-HSQC spectra, the amide hydrogen region is resolved in a second dimension and broad peaks are translated into dispersed NH resonances.

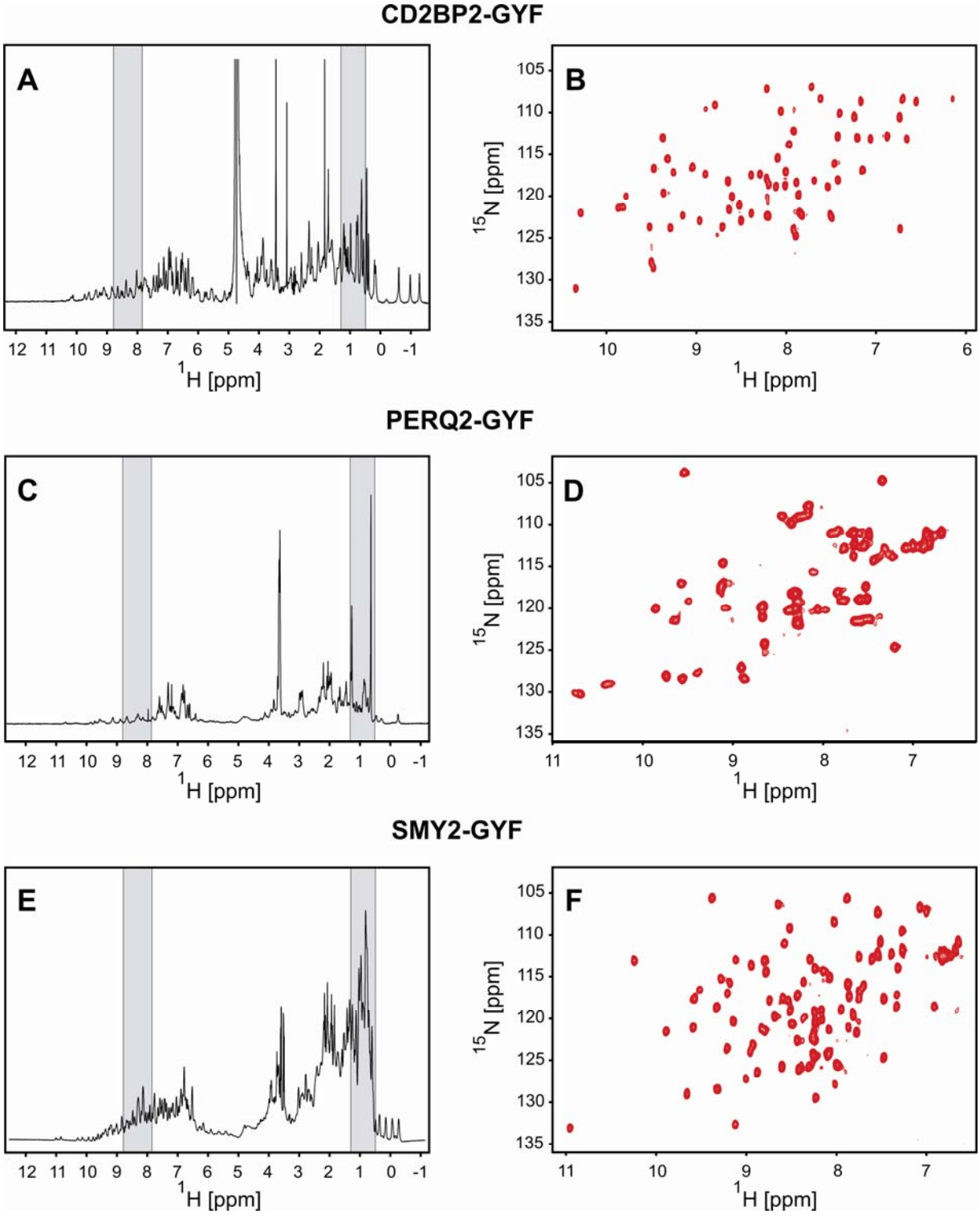

Fig. 5.1: NMR spectra of the GYF domains of CD2BP2, PERQ2, and SMY2
^{1}H and ^{1}H-^{15}N-HSQC spectra of CD2BP2- (A, B), PERQ2- (C, D), and SMY2-GYF (E, F), respectively. The NMR samples of CD2BP2-GYF were buffered with 50 mM Na-phosphate, pH 6.3, those of PERQ2- and SMY2-GYF with PBS. The one- and two-dimensional spectra were recorded at the following conditions respectively: CD2BP2-GYF 0.1 mM, 298 K and 0.2 mM, 297 K; PERQ2-GYF 0.2 mM, 297 K and 0.6 mM, 296 K; and SMY2-GYF 1.2 mM, 299 K and 0.2 mM, 297 K. The shaded regions in the ^{1}H spectra indicate the random coil regions of backbone amide (left) and aliphatic protons (right).

For the GYF domain of SMY2, the NH resonances in the ^{1}H-^{15}N-HSQC spectrum were well dispersed, as they were for CD2BP2-GYF, further indicating a native fold (Fig. 5.1b and f). Resonance dispersion of PERQ2-GYF also confirmed the folding of this domain. Substantial peak overlap in the upfield region, however, predicted dimerization or oligomerization of the domain (Fig. 5.1d), possibly due to the presence of the His_6-tag, which lacked in the other two GYF domain constructs.

5.2 Binding Test of GYF Domains to Immobilized Peptides

To test the functionality of the CD2BP2-, PERQ2-, SMY2-, and SYH1-GYF domains as GST-fusions and in the context of peptide SPOT arrays, the GST-tagged domains were incubated with peptides synthesized on cellulose membranes. Synthetic peptides comprised the known CD2BP2-GYF binding sites in CD2 and PRS in the interaction candidate MSL5 for SMY2 and SYH1. Since no preliminary interaction candidates for PERQ2-GYF were known, this GST-fusion construct was examined for binding to proline-rich peptides from human CD2 and some of its mammalian homologs. A PRS of PERQ1 and an internal PRS of PERQ2 were also included.

All GST-GYF domain fusion constructs bound to several peptides on the membranes (Fig. 5.2). CD2BP2-GYF encountered CD2 derived peptides comprising both the double and single binding motif (Fig. 5.2a, peptides 1 and 4), but not the scrambled CD2 peptides (peptides 2, 3, 5, and 6). These preliminary binding experiments established that SPOT peptide arrays were a suitable method to investigate GYF domain interactions. Detectable binding of the other GYF domains approved their anticipated functionality and correct folding. For the two *Saccharomyces cerevisiae* GYF domains, all identified binding sites in MSL5 (Fig. 5.2b, peptides 9, 11–13, 16, 19, and 20) coincided with the presence of the sequence motif PPGL. PERQ2-GYF bound to the CD2BP2-GYF interaction sites in CD2 molecules from different species. All binding peptides comprised the motif PxPPGH(H/R) as a common element (Fig. 5.2c, peptides 25–28 and 30). A direct contribution to binding could only be attributed to the glycine of the motif. Substitution of serine for glycine abolished binding (compare binding peptides 25–28 and 30 with peptide 29). Sequence similarity of the CD2-PRS prevented further conclusions to be drawn about the importance of other positions in the motif for PERQ2-GYF binding.

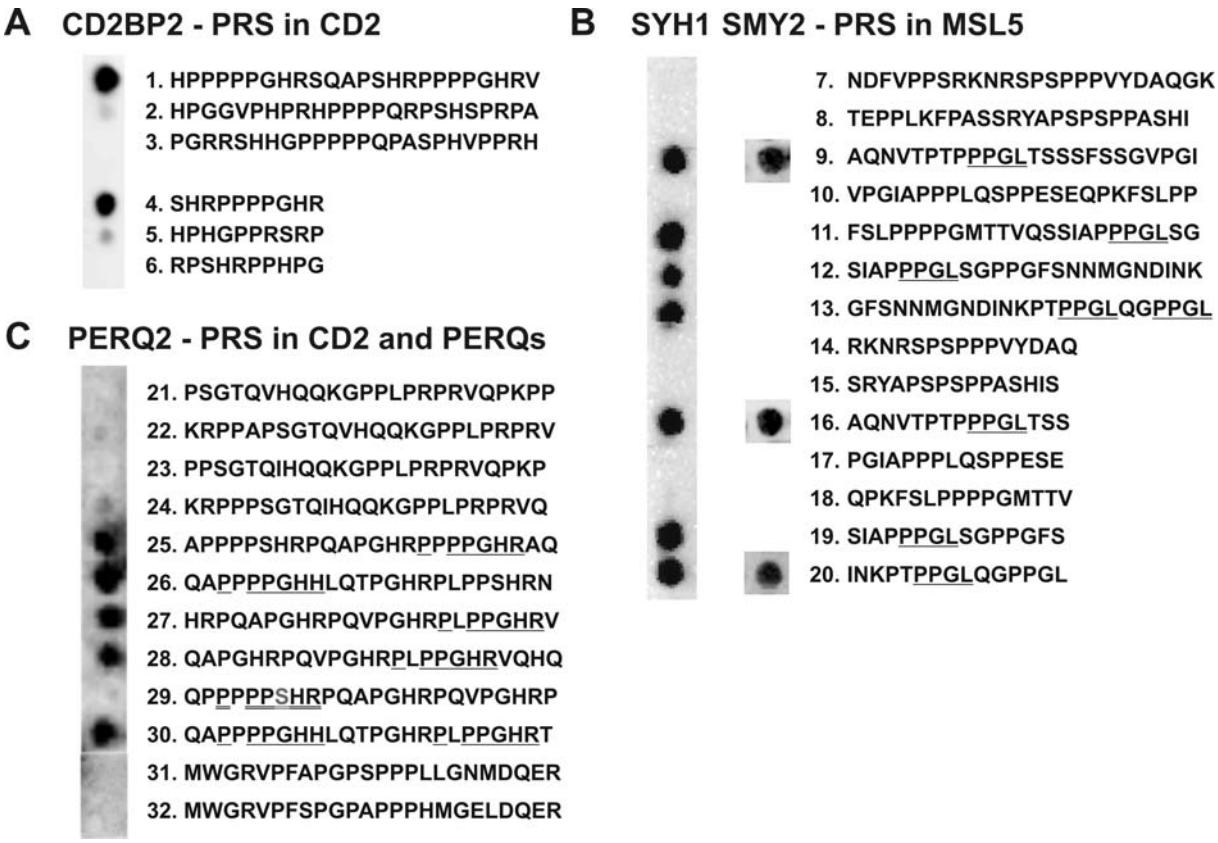

Fig. 5.2: Binding test of GYF domains to peptides on SPOT membranes
GST-fusion constructs of CD2BP2-, SMY2-, SYH1-, and PERQ2-GYF were tested for binding to PRS synthesized on cellulose membranes. (A) The GYF domain of CD2BP2 was tested for binding to the interaction site in CD2 (peptides 1 and 4). Peptides 2, 3, 5, and 6 are scrambled from peptides 1 and 4, respectively, and served as negative control. (B) The GYF domains of the two yeast paralogs were incubated with membrane bound proline-rich peptides from MSL5 (peptides 7–20). (C) The membrane for PERQ2-GYF comprised proline-rich peptides from human (peptides 21, 22), mouse (peptides 23, 24, and 30), cat (peptide 25), rat (peptide 26), and horse (peptides 27–29) CD2 cytoplasmic tails as well as from human PERQ1 (peptide 31) and PERQ2 (peptide 32). Sequences of peptides are given and suggested binding motifs are underlined. The closely related non-binding variant in peptide 29 is double-underlined, and the differential residue is shown in grey. Peptide-bound domains on the membranes were detected using anti-GST primary and HRP coupled secondary antibodies along with a chemiluminescence substrate.

5.3 Set up of Phage Display Experiments with GYF Domains

Compatibility of the phage display system with GYF domain–peptide interactions was studied using GST-tagged GYF domains of CD2BP2, SYH1, and SMY2 (Fig. 5.3). The presence of peptides on the phage surface was exemplified for the FLAG-tagged CD2 peptide SHRPPPPGHRVQ (Fig. 5.3a and b). Different phage constructs (Fig. 5.3a), representing single and double binding motifs of CD2 or MSL5 on the surface, respectively, were then tested for binding to GST-GYF proteins immobilized on glutathione-sepharose 4B beads. Stronger binding correlates with higher phage titers in the eluates from immobilized proteins. MSL5-PRS presenting phage particles (MSL5S and MSL5L) were significantly enriched (more than 10 fold)

in eluates from SMY2- and SYH1-GYF, compared to GST alone (Fig. 5.3c). For wild-type phage (WT), GST and the two yeast GST-GYF fusions behaved similarly. These results showed that binding properties of the GYF domain family could be analyzed by phage display. The CD2-PRS presenting phage constructs for CD2BP2-GYF, however, failed to reveal clear domain specific binding (Fig. 5.3d). No significant CD2BP2-GYF dependent increase in the elution titers was observed using phages CD2-FLAG, CD2S, and CD2L, although phage CD2L bound slightly better to the GYF construct than to GST. Phage display was nevertheless performed with CD2BP2-GYF (Chapter 8). Subsequent analysis indicated that phages, displaying higher affinity binding peptides (phages #26, #27, and #37, obtained after three rounds of panning; see Table 8.1 and Fig. 5.3a), resulted in selective enrichment on CD2BP2-GYF compared to GST alone (Fig. 5.3d). The inability of phages, presenting CD2 derived motifs, to enrich significantly on CD2BP2-GYF loaded beads could be due to the low binding affinity, at least for the single motif (~ 190 μM; Chapter 8). The reasons for the longer CD2 peptide to fail in phage display experiments despite an apparent affinity of 10–40 μM[23] (Chapter 8) remain elusive. Possibly mass transport limitations of the two interaction partners (GST-GYF domains, bound to beads and peptides on phage particles), could interfere with avidity effects of the tandem binding motifs in the longer CD2 peptide. Thereby, the apparent affinity could be reduce below the threshold which is required for efficient enrichment. Alternatively, longer peptides might be presented less efficiently or they are partially degraded. This could prevent enrichment of peptides comprising the lower affinity binding motifs in CD2, while enrichment of the higher affinity peptides of MSL5 (Table 9.4) would be less affected.

The conducted experiments attested the GYF domains of CD2BP2, PERQ2, and SMY2 to be folded and the GST-tag did not interfere with binding. Correct folding of the SYH1-GYF domain was assumed because of the sequence similarity to SMY2 (67 %) and its binding competence in SPOT analysis and phage display experiments (see Fig. 5.2 and Fig. 5.3). No preliminary experiments for the *Arabidopsis thaliana* GYF domain of GYN4 were performed, but the homologous Q9FZJ2 GYF domain of the same organism (69 % similarity) was found to be folded (data not shown). The other domains under investigation, Q9VKV5-GYF from *Drosophila melanogaster* and yeast LIN1-GYF, both belong to the CD2BP2 subfamily of GYF domains. Expression and stability of the LIN1 construct were too low for binding studies, although different constructs with varying domain borders were tested (see Table 4.2).

The GST-fusion of Q9VKV5-GYF expressed well and was stable but failed to provide valuable data in both phage display and SPOT analysis experiments (data not shown). An explanation for the inability of Q9VKV5-GYF to reveal binding could be misfolding of the domain. Partial

degradation during purification cannot be ruled out since masses of GST-fusion proteins were roughly estimated from SDS-polyacrylamide gels only (data not shown). This limited the analysis of the first subfamily to CD2BP2-GYF.

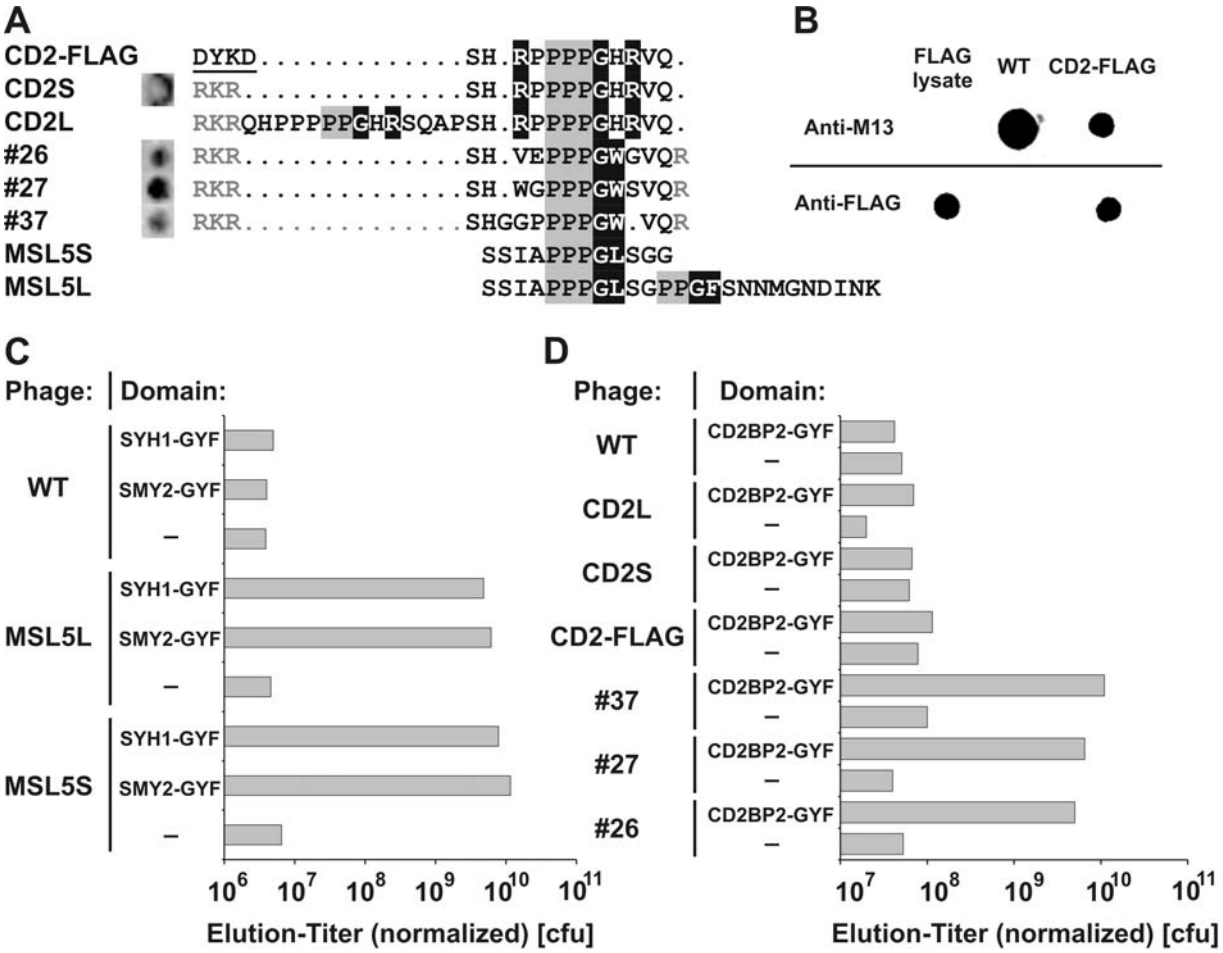

Fig. 5.3: Phage display test

(A) Phages used to evaluate the phage display system. The phage constructs CD2S, CD2L, MSL5S, and MSL5L present the single and double binding motif of CD2 or MSL5 on the phage surface, respectively. Phage CD2-FLAG is the FLAG tagged version of CD2S, phages #26, #27, and #37 were obtained after three rounds of panning using the focused library and CD2BP2-GYF (results from Table 8.1). Spots revealed binding of CD2BP2-GYF to the peptides, when synthesized on a membrane. The shortened FLAG epitope is depicted in underlined letters; residues introduced to compensate for negative charges flanking the insertion point in the g8 protein are shown in grey. The triple proline region, defined in the focused library and proline residues in binding sites of natural proteins are on grey background. Additional residues, belonging to the GYF recognition motifs are represented as white letters on black background (residues belonging to the GYF recognition motifs are described in Chapter 6, 8, and 9). (B) Test of surface presentation of peptides by phages. CD2-FLAG and wild-type (WT) phages as well as lysate of cells expressing FLAG-tagged protein (FLAG lysate, positive control) were spotted onto a membrane and incubated either with anti-M13 antibody (top row), which recognizes an epitope in g8p, or anti-FLAG antibody (bottom row). Primary antibodies were detected with a HRP coupled secondary antibody and a chemiluminescent substrate. (C, D) Results of phage selection on immobilized GST protein (–) or the GST-fusions of SMY2-, SYH1- (C), and CD2BP2-GYF (D). Elution titers are normalized to equal input titers of 10^{11} colony forming units (cfu).

The presence of an internal PRS had no effect on protein stability for GST-tagged GYN4- and SYH1-GYF. However, removal of the tag from GYN4- and SYH1-GYF, comprising the PRS, did not result in soluble domains (data not shown). Stabilizing effects of the GST moiety were reasoned to support solubility of the respective GYF constructs. Correspondingly, fluorescence titrations had to be performed with the GST-tagged versions in the case of GYN4-GYF (see Fig. 9.8).

The preliminary interaction studies established the binding competence of several GYF domain constructs and set the basis for systematic analysis of recognition specificities of GYF domains from CD2BP2, PERQ2, SMY2, SYH1, and GYN4 (Chapters 6, 8, and 9). Additionally, the experiments revealed recognition motifs for SMY2-, SYH1-, and PERQ2-GYF and reconfirmed the known interaction site for CD2BP2-GYF. Supporting evidence for binding of SMY2 and SYH1 to MSL5[248] and CD2BP2 to CD2[23,42] led to a closer inspection of these recognition motifs (see Chapters 6 and 9.1).

CHAPTER 6

Recognition Sequences for the GYF Domain Reveal a Possible Spliceosomal Function of CD2BP2

Michael Kofler, Katja Heuer, Tobias Zech, and Christian Freund

Journal of Biological Chemistry (2004); **279** (27): 28292–7.
The article can be obtained from www.jbc.org.

Contributions:
Dr. Katja Heuer performed the pulldown experiment. Tobias Zech did the SmB/B'-CD2BP2 colocalization studies[296]. Membranes were obtained from Angelika Ehrlich and Dr. Rudolph Volkmer-Engert. Annerose Klose, Dagmar Krause, and Dr. Michael Beyermann synthesized the peptides used in this study.

Remarks :
Sequences of peptides on membranes, depicted in Fig. 6.7, are listed in the supplementary Table 12.1.
Figures in the publication lack chapter numbers. References to these figures throughout the remaining thesis text retain the same numbering, with the Chapter number as prefix (e.g. Fig. 5 in this publication is referred to as Fig. 6.5 in the remaining text).

Corrections:
CD2BP2 is a component of the U5, not the U2 snRNP (page 66).

6.1 Colocalization Studies of CD2BP2 and CD2 in HeLa Cells

Expression of EGFP-CD2BP2 in HeLa S3 and Jurkat J77 cells revealed a predominant nuclear localization, supporting a possible interaction with SmB/B' (Fig. 6.6). Additional colocalization experiments should clarify whether CD2 overexpression could direct CD2BP2 to the membrane. Therefore, full-length CD2 or a deletion mutant, lacking the entire cytoplasmic tail (CD2taa236) were expressed in HeLa S3 cells, together with EGFP-CD2BP2. Neither the deletion mutant nor full-length CD2 affected the nuclear localization of CD2BP2 and no obvious association with the membrane was observed (Fig. 6.8).

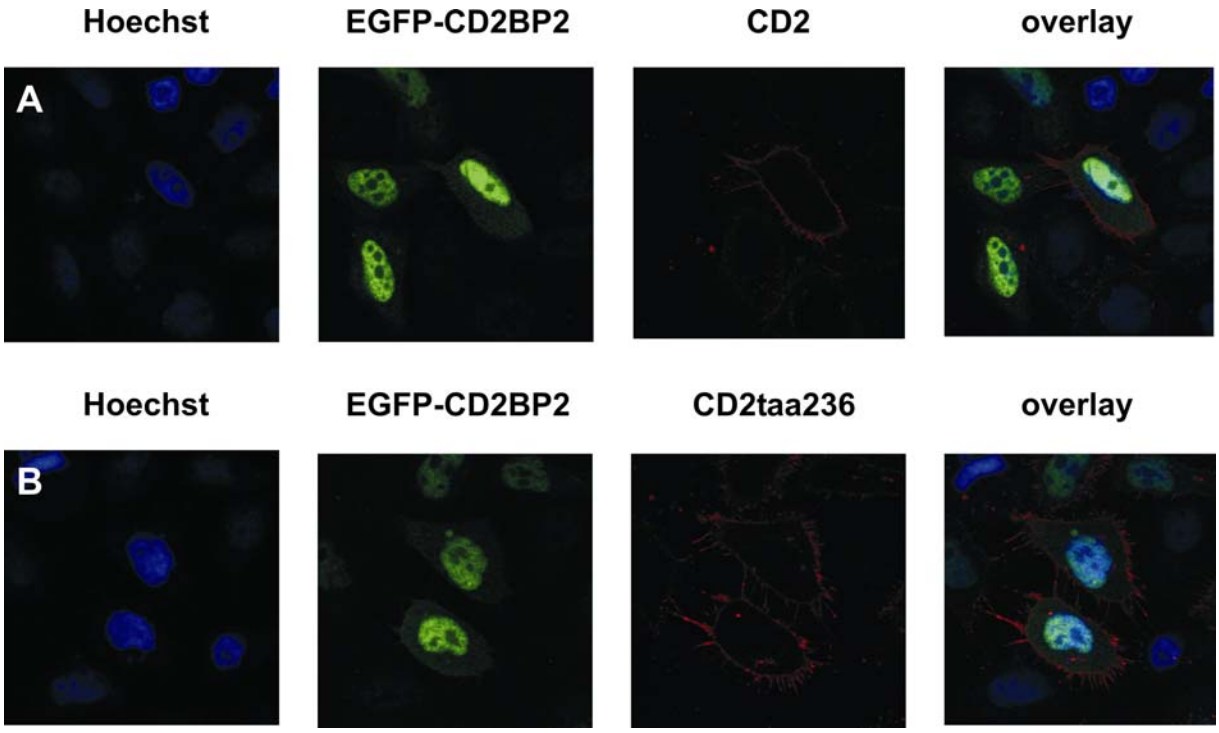

Fig. 6.8: Effect of CD2 overexpression on CD2BP2 localization in HeLa cells
HeLa S3 cells transiently expressing EGFP-CD2BP2 and either CD2 (A) or a deletion variant lacking the cytoplasmic tail (CD2taa236), (B) were fixed 48 h after transfection. Nuclei were stained with Hoechst 33258 dye, CD2 and CD2taa236 were detected with mouse $T11_1$ primary and a Cy3-coupled anti-mouse secondary antibody. Laser confocal images reveal CD2BP2 to localize predominantly to the nucleus, irrespective of the expressed CD2 variant.

These results question a direct interaction of CD2 and CD2BP2 at the cytoplasmic membrane. A reason for the plaucity of CD2BP2 membrane localization in the presence of CD2 could be inaccessibility of the CD2 cytoplasmic tail. In fact, for the CD3ζ cytoplasmic tail, lipid binding was found to regulate its accessibility *in vitro*[311]. The CD3ζ intracellular domain binds to acidic lipid vesicles and thereby adopts a helical conformation. The interaction prevents

phosphorylation of immunoreceptor tyrosine-based activation motifs (ITAMs) in CD3ζ *in vitro*. Phosphorylated CD3ζ-tail, on the other hand, does not bind to vesicles[311]. According to the suggested model, TCR clustering limits the accessible membrane surface for the CD3ζ cytoplasmic tails. Dissociation from the membrane allows Lck to phosphorylate the otherwise blocked ITAMs which then represent stable docking sites for other signaling proteins. Recruitment of signaling proteins to the phosphorylated ITAMs initiates downstream signaling cascades. For CD2, a similar scenario is plausible. The CD2 intracellular domain is highly basic (net charge of + 14) and clustering upon CD58 binding might alleviate its membrane association, triggering binding of PRD to the accessible PRS. However, CD2 lacks any aromatic residues which might be important for membrane association and no data concerning lipid binding of the CD2 tail is available yet.

CHAPTER 7

Alternative Binding Modes of Proline-Rich Peptides Binding to the GYF Domain

Wei Gu, Michael Kofler, Iris Antes, Christian Freund, and Volkhard Helms
Biochemistry (2005); **44** (17): 6404–15.
The article can be obtained from pubs.acs.org.

Contributions:
All molecular dynamics simulations were performed by Wei Gu and Dr. Iris Antes. I did the NMR titration and SPOT analysis experiments. Membranes were obtained from Angelika Ehrlich. Annerose Klose, Dagmar Krause, and Dr. Michael Beyermann synthesized the peptides used in this study.

Remarks :
Figures in the publication lack chapter numbers. References to these figures throughout the remaining thesis text retain the same numbering, with the Chapter number as prefix (e.g. Fig. 4 in this publication is referred to as Fig. 7.4 in the remaining text).

CHAPTER 8

Novel Interaction Partners of the CD2BP2-GYF Domain

Michael Kofler, Kathrin Motzny, Michael Beyermann, and Christian Freund
Journal of Biological Chemistry (2005); **280** (39): 33397–402.
The article can be obtained from www.jbc.org.

Contributions:
Membranes were obtained from Angelika Ehrlich. Annerose Klose, Dagmar Krause, and Dr. Michael Beyermann synthesized the peptides used in this study.

Remarks :
A supplementary figure is attached to the article. It depicts Fig. 8.3 with dot numbers referring to the supplementary Table 12.2.
Figures in the publication lack chapter numbers. References to these figures throughout the remaining thesis text retain the same numbering, with the Chapter number as prefix (e.g. Fig. 3 in this publication is referred to as Fig. 8.3 in the remaining text).

Corrections:
The focused library is of the format RKRSHXXPPPXXXVQR (page 85 and 86).
High stringency media is deficient for adenine (Ade) in addition to His, Leu, and Trp (see Chapter 4.15), not alanine (page 86).

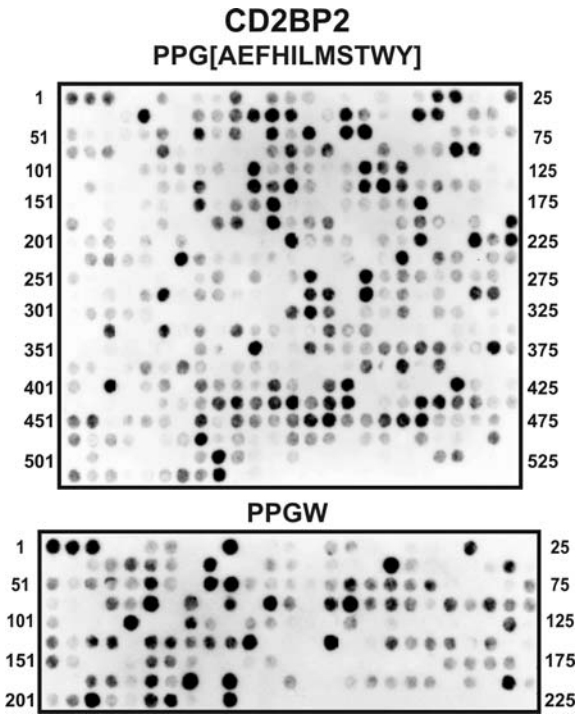

Supplemental to Fig. 8.3: Identification of CD2BP2-GYF PPGW class binding sites of the human proteome

Swiss-Prot and TrEMBL databases were searched for sequences meeting the relaxed and strict consensus motif for CD2BP2-GYF binding, respectively. The corresponding sequences were synthesized on membranes and tested for CD2BP2-GYF binding as described in Fig. 8.2. Consensus sequences applied for the searches are depicted above the membranes (upper membrane: relaxed consensus, lower membrane: strict consensus). The relaxed consensus had to be present twice in the protein with a maximal distance of 40 amino acids in order to be selected for synthesis on a membrane. The figure is identical to Fig. 8.3, but comprises dot numbers, referring to the peptide sequences in Table 12.2.

8.1 Identification of Interaction Sites in Viral Proteins

The different interaction partners of the GYF domain in CD2BP2 link the protein to spliceosomal functions and signal transduction in T cells. In addition to the endogenous interaction partners that are present in the human proteome, exogenous binders might exist that are derived from intracellular parasites. In the case of EVH1[54,312], UEV[60,313], and WW[314-316] domains, bacterial and viral proteins were identified to specifically bind to these PRD and to utilize the binding function for the benefit of the parasite. Exploitation of CD2BP2 by pathogen proteins could optimize splicing processes for viral gene expression or genome amplification. Human immunodeficiency viruses (HIVs) for example, could interfer with CD2-mediated T cell stimulation as important step for their life cycle.

To account for such possible interaction partners, the Swiss-Prot and TrEMBL databases were searched for viral proteins comprising the motif PPG[AEFHILMSTVWY]. 383 peptides were found to meet the search criteria. Peptides, synthesized on a membrane, were incubated with CD2BP2-GYF. Several sequences revealed binding (Fig. 8.6). One interesting candidate is the protein Vpx from HIV type 2 (HIV-2) and simian immunodeficiency viruses (SIVs)[317,318]. The C-terminus of the protein comprises a PPGL motif and was found four times (boxed and circled dots) amongst the eleven peptides with highest Boehringer light unit (BLU) values. A possible implication in viral replication would be an interesting aspect of CD2BP2 functions.

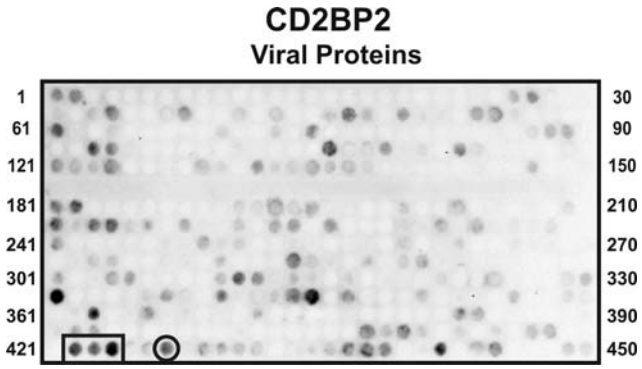

Fig. 8.6: Identification of CD2BP2-GYF binding sites in viral proteins
Swiss-Prot and TrEMBL databases were searched for viral protein sequences comprising the relaxed consensus PPG[AEFHILMSTVWY] for CD2BP2-GYF. The corresponding peptides were synthesized on a membrane and tested for CD2BP2-GYF binding as described in Fig. 6.2. Numbers refer to the peptide sequences listed in Table 12.3. Amongst the eleven peptides with the highest BLU values, three are derived from the Vpx protein of different HIV strains (boxed dots), one from the homologous protein in SIV (circled dot).

CHAPTER 9

GYF Domain Proteomics Reveals Interaction Sites in Known and Novel Target Proteins

Michael Kofler, Kathrin Motzny, and Christian Freund

Molecular and Cellular Proteomics (2005); **4** (11): 1797–811.
The article can be obtained from www.mcponline.org.

Contributions:
Membranes were obtained from Angelika Ehrlich. Annerose Klose, Dagmar Krause, and Dr. Michael Beyermann synthesized the peptides used in this study.

Remarks :
Sequences of peptides on membranes, depicted in Fig. 9.3, are listed in the supplementary Table 12.4. The chemical shifts of SMY2-GYF NH backbone groups are listed in Table 12.5 and an assigned ^{1}H-^{15}N-HSQC spectrum is depicted in Fig. 12.1.
Figures in the publication lack chapter numbers. References to these figures throughout the remaining thesis text retain the same numbering, with the Chapter number as prefix (e.g. Fig. 2 in this publication is referred to as Fig. 9.2 in the remaining text).

Corrections:
For the production of labeled protein, minimal medium A, supplemented with $^{15}NH_4Cl$ or both $^{15}NH_4Cl$ and [^{13}C] glucose was used (page 96). The focused library is of the format RKRSHXXPPPXXXVQR (page 96 and 98). The SMY2 start site has been moved 50 codons downstream on September 22 2003. The numbers, indicating the position of the depicted fragment within full-length SMY2, refer to the old start site (page 97).

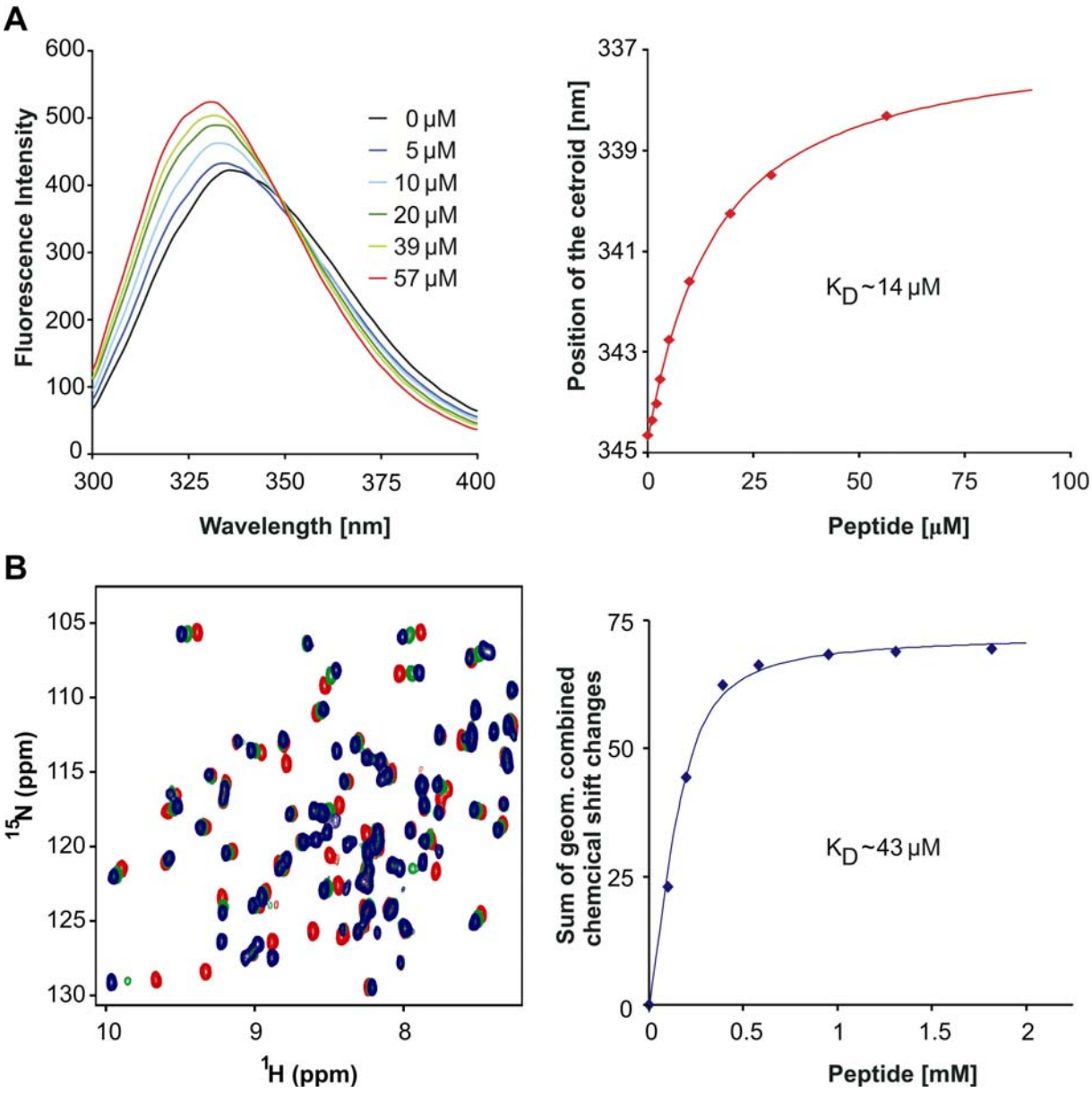

Fig. 9.9: Supplementary figure—Raw data and deduced titration curves using fluorescence and NMR spectroscopy, as exemplified for the SMY2-GYF domain and the peptide MSL5S1

(A) Fluorescence titration of the SMY2-GYF domain with the peptide MSL5S1. In the presence of increasing peptide concentrations, fluorescence was excited at 280 nm and emission spectra (300–400 nm) were recorded (left). The position of the centroid during titration was plotted against the ligand concentration (right) and a dissociation constant was calculated assuming a two-state binding model. (B) NMR titration of the same protein-peptide pair as in (A). The chemical shift changes of the NH resonances upon addition of increasing amounts of MSL5S1 peptide were detected by overlaying the recorded ^{1}H-^{15}N-HSQC spectra. The central region of the spectra of the isolated SMY2-GYF domain (red), SMY2-GYF in the presence of an equimolar concentration of MSL5S1 peptide (green), and in the presence of a tenfold excess of MSL5S1 peptide (blue) are superimposed and shown on the left. ^{1}H and ^{15}N components of the shift changes were geometrically (geom.) combined to obtain the total shift change value for each resonance according to Chapter 3.2. The sum of the geometrically combined chemical shift changes of all resonances were plotted against the ligand concentration (right) and a dissociation constant was calculated as in (A).

9.1 Evaluation of Binding Motifs in Suggested Interaction Partners

The importance of individual positions in the recognition motif PPGΦ of the four SMY2-type GYF domains was clearly demonstrated for phage display derived ligands (Fig. 9.2). Alanine scans and substitution analysis of consensus binding sites from the approved ligand MSL5 for SYH1-GYF and from the proposed interaction partners AKNA and SWAN for PERQ2-GYF

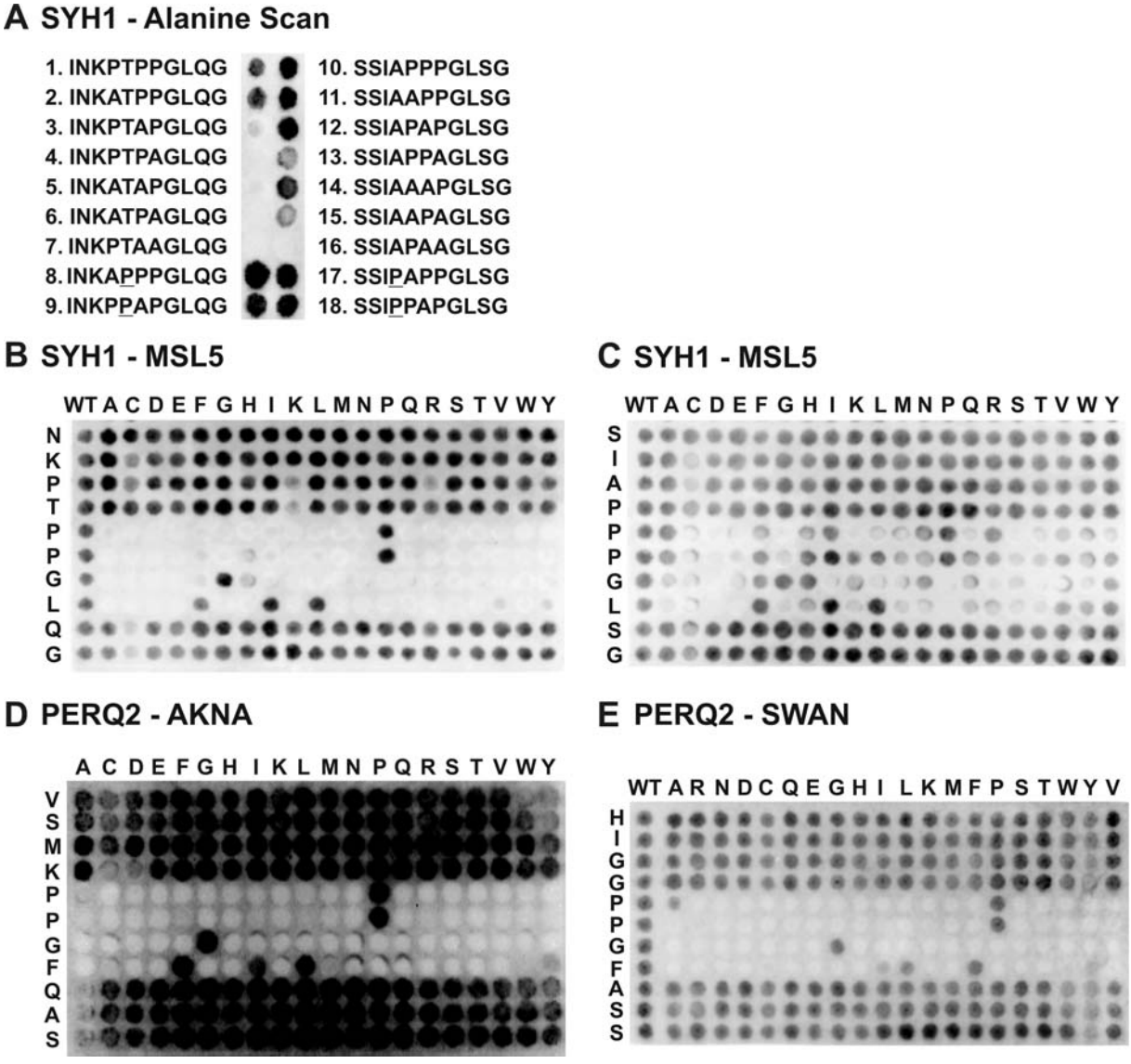

Fig. 9.10: Alanine scan and substitution analysis of peptides form natural proteins
(A) Alanine scans and (B and C) substitution analysis of binding sequences of the identified SYH1-GYF interaction partner MSL5. (D and E) Substitution analysis of binding sequences of the proposed PERQ2-GYF interaction partners AKNA and SWAN. In the alanine scan experiments, single or multiple proline residues in the peptides were replaced by alanine. Underlined prolines replaced wild-type residues. Organization of the substitution analysis membranes and detection of binding is described in Fig. 9.2. Membranes were incubated with GST-fusions of SYH1-GYF (A, B, and C) or PERQ2-GYF (D and E).

reconfirmed these findings for native peptide ligands (Fig. 9.10). Replacement of a proline in the PPGL motif of the peptide INKPTPPGLQG from MSL5 interfered with binding to SYH1-GYF (Fig. 9.10a, peptides 1–7). Elongation of the proline-rich stretch (underlined prolines in Fig. 9.10a, peptides 8 and 9) alleviated the requirement of specific amino acid positioning in the recognition signature (compare peptides 3 and 9 in Fig. 9.10a). In the MSL5 peptide MSL5S1 (SSIAPPPGLSG), the consensus was even more permissive for amino acid exchanges (Fig. 9.10a, c). The loss of binding energy upon replacement of residues within the recognition motif in these ligand–domain complexes is probably compensated for by stabilization of the PPII-helix and additional interactions with flanking residues. The relative high affinity (~ 13 μM for both yeast GYF domains, see Table 9.4) supports the hypothesis of additional, favourable interactions between the MSL5S1 peptide and SYH1-GYF. These findings highlight the influence of flanking regions on the recognition signature. Exchanges of residues, even in key positions, without detectable decrease in binding affinity is plausible in aa otherwise favourable sequence context. Such alterations limit the utility of consensus motif-based screening approaches. Consequently, yeast two-hybrid screens complemented the knowledge-driven experiments, but did not reveal additional binding sites (see Table 9.3).

Investigation of the interaction between the peptide VSMKPPGFQAS from AKNA and PERQ2-GYF by NMR titration revealed distinct NH resonance shifts without changing the region of large peak overlap (Fig. 9.11b). Initial NMR spectra of PERQ2-GYF were interpreted to reveal a folded yet di- or oligomerized domain (Chapter 5.1 and Fig. 5.1). The titration results corroborated this assumption. A transition from an unfolded to a folded state or resolution of aggregates upon ligand addition would reduce peak overlap in the spectra, which was not observed. Rather the association state of PERQ2-GYF is independent of and does not interfere with ligand binding. The structure of CD2BP2-GYF in complex with the protein U5-15K (Fig. 1.4 and Fig. 11.1) clearly identifies the C-terminal half of the domain, opposite the PRS binding epitope, as interaction site. It is tempting to assume the same region of PERQ2-GYF to be involved in protein-protein interactions and to be the reason for di- or oligomerization.

Fig. 9.11: PERQ2-GYF NMR titration experiments

NMR titration of PERQ2-GYF with the binding peptide from AKNA (B). For comparison, titration results of CD2BP2-GYF with the peptide SmB-2 from Fig. 6.4 (A) and of SMY2-GYF with the peptide MSL5L2 from Fig. 9.7 (C) are depicted. Upon addition of increasing amounts of peptide, the resonances of GYF domains shift gradually. ^{1}H-^{15}N-HSQC spectra of CD2BP2- and SMY2-GYF with a peptide : domain ratio of 0, 0.5, 1, and 10 are depicted in red, green, gold, and blue, respectively. Similarly colored spectra of PERQ2-GYF correspond to ratios of 0, 0.33, 0.66, and 3.3. Conditions of the NMR measurements are indicated in Fig. 5.1.

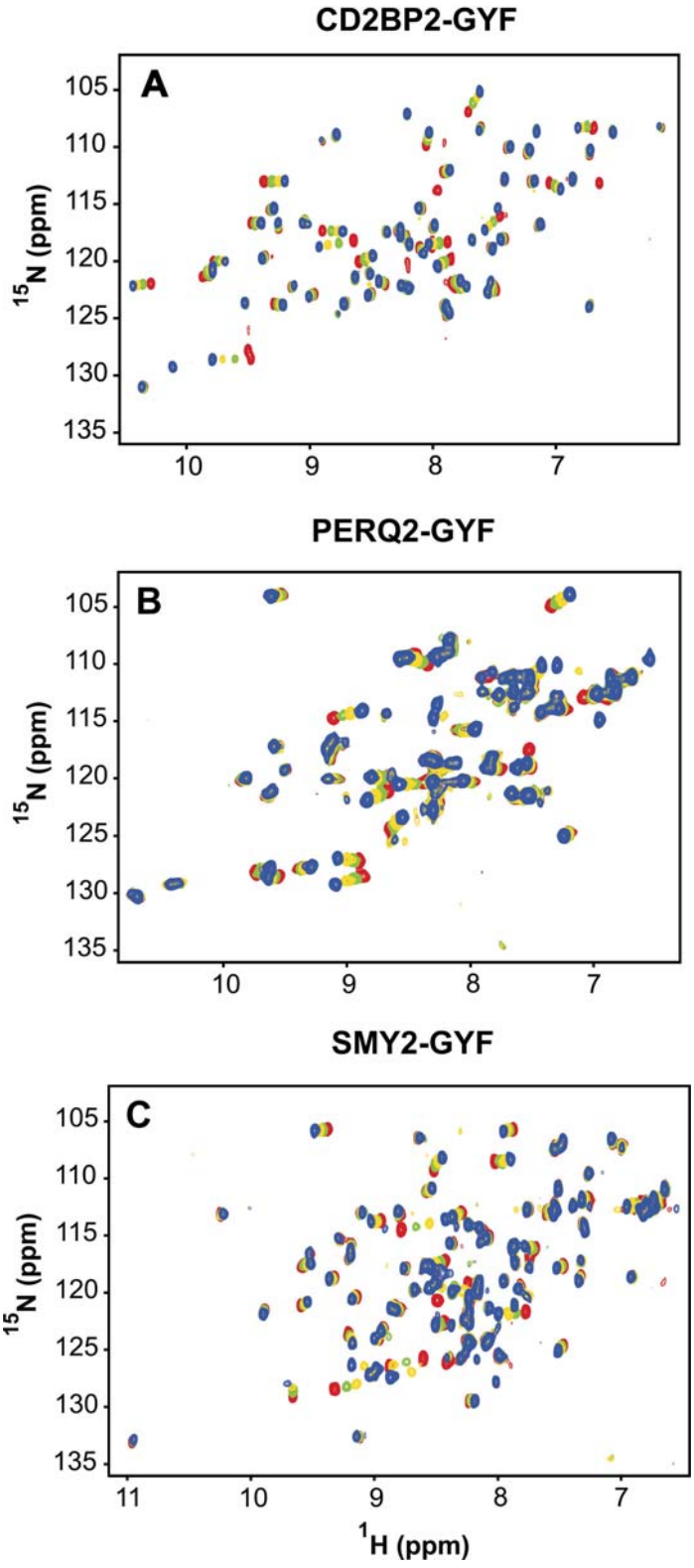

CHAPTER 10

Review: The GYF Domain

Michael Kofler and Christian Freund

FEBS Journal (2006); Jan, **273**: 245–256.

The article can be obtained from www.febsjournal.org.

Remarks :

Figures in the publication lack chapter numbers. References to these figures throughout the remaining thesis text retain the same numbering, with the Chapter number as prefix (e.g. Fig. 1 in this publication is referred to as Fig. 10.1 in the other chapters).

Corrections:

The PRS of PI31 is recognized by both CD2BP2- (Chapter 8) and PERQ2-GYF (data not shown) and should therefore be depicted in bold letters in Table 10.1 (page 123).